

Solution Electron Affinity Perturbation Due to the Deuteration of [16]Annulene

Todd L. Kurth,[†] Eric C. Brown,[†] Alex I. Smirnov,[‡] Richard C. Reiter,[†] and Cheryl D. Stevenson^{*,†}

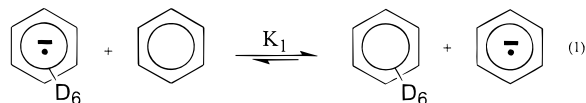
Department of Chemistry, Illinois State University, Normal, Illinois, 61790-4160, and Illinois EPR Research Center, University of Illinois at Urbana–Champaign, Urbana, Illinois 61801

Received: August 9, 1999

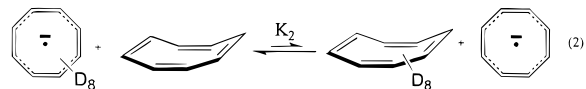
X-Band (9.8 GHz) EPR measurements show that the free energy change controlling the electron transfer from the anion radical of perdeuterated [16]annulene to neutral [16]annulene ($C_{16}D_{16}^{\bullet-} + C_{16}H_{16} \rightleftharpoons C_{16}H_{16}^{\bullet-} + C_{16}D_{16}$) is $\Delta G^\circ = -0.65$ kcal/mol. When supplied with vibrational frequencies from B3LYP/6-31+G* calculations, the QUIVER program determines a ΔG° value of -0.142 kcal/mol. Thus, the experimental and theoretical values are in qualitative agreement. This result is the opposite of that obtained for the [8]annulene system, where the solution electron affinity of C_8D_8 proved to be slightly greater than that for C_8H_8 . 1H NMR (400 MHz) experiments reveal that the barrier to ring flattening is greater in the $C_{16}D_{16}$ system than in the $C_{16}H_{16}$ system. Coupled with the DFT prediction that the $C_{16}D_{16}^{\bullet-}$ is nearly planar, this accounts for the equilibrium isotope effect observed in the electron transfer. The W-Band (94 GHz) EPR spectra, showing that the isotropic g -factor of the [16]annulene anion radical is not altered via perdeuteration, further support a nearly planar $C_{16}D_{16}^{\bullet-}$. The DFT calculations also predict that the dianion of [16]annulene is completely planar. However, deuteration of all but one of the hydrogens in $C_{16}H_{16}^{2-}$ results in an upfield chemical shift of 0.086 ppm for the internal proton resonance at 153 K. This increase in ring current (π -delocalization) is accounted for in terms of a C–C=C bond angle (σ -framework) relaxation, as shorter C–D bonds attenuate the internal steric interactions in $C_{16}D_{15}H^{2-}$.

Introduction

It has been shown for a variety of polyaromatic hydrocarbons (PAH) that the solution electron affinity of a deuterated system is significantly lower than that of its perprotiated analogue.¹ Not atypical is the benzene system for which the equilibrium constant for electron transfer is $K_1 = 3.85$ at 173 K. This

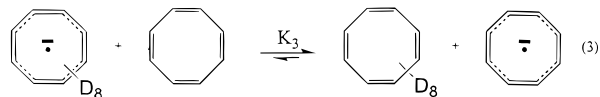


corresponds to a normal standard free energy change, in which the perprotiated analogue “prefers” the electron, $\Delta G^\circ_1 = -0.463$ kcal/mol.¹⁶ The sign and magnitude of ΔG°_1 have been explained in terms of zero point energy (ZPE) changes that occur upon deuteration.^{1a} The change in free energy for the analogous electron-transfer involving cyclooctatetraene (COT), reaction 2,

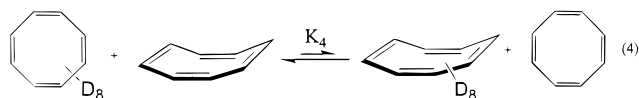


is the inverse (the deuterated material prefers the electron). It is also smaller in magnitude than the free energy change for benzene and other PAH systems.¹ At 173 K, $K_2 = 0.86$, which corresponds to a ΔG°_2 of 0.05 kcal/mol.²

The Bigeleisen equation,³ when supplied with vibrational frequencies obtained from density functional theory (DFT) calculations, accounts for the observed equilibrium isotope effect (EIE) in reaction 1.⁴ Analogously, these calculations predict that, when the COT system is constrained to planarity, the EIE on the electron transfer of reaction 3 is large and normal; $K_3 = 3.0$ at 173 K, $\Delta G^\circ_3 = -0.38$ kcal/mol.⁴ In agreement, 1H NMR



observations, of the isopropoxy–COT system, show a significant inverse isotope effect upon the flattening of the tub-shaped COT ring system; the activation energy of ring flattening for the deuterated material is lower.⁵ Thus, both experiment and theory indicate that the small inverse EIE for reaction 2 is attributable to the contribution of a large inverse EIE on the planarization of COT, reaction 4; $K_4 = K_2/K_3 = 0.29$ at 173 K and $\Delta G^\circ_4 = 0.43$ kcal/mol.⁵



ZPE arguments justify the inverse EIE in reaction 4.^{4,5} The tub D_{2d} geometry of COT has lower bond vibrational frequencies than those of the planar D_{4h} . Upon electron addition, planarization to the D_{4h} structure occurs, and the resulting vibrational partition function renders the $D_{2d} \rightarrow D_{4h}$ conformation change less unfavorable in the perdeuterated system.⁴ Thus, the distur-

* To whom correspondence should be addressed.

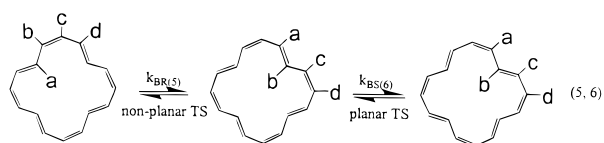
[†] Illinois State University.

[‡] University of Illinois.

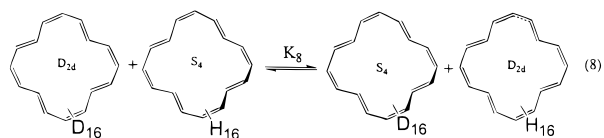
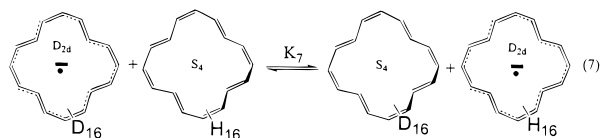
tion from the ground state geometry of the COT system, caused by electron addition, takes place with proportionately less resistance in the isotopically heavy system.⁴

This effect could, in principle, play a role in the planarization of the larger annulenes. For example, neutral [16]annulene primarily exists in a nonplanar geometry and acquires a more planar geometry upon the addition of an odd electron.^{6a} It is reasonable to expect that this planarization will contribute to an EIE for the electron transfer between perdeuterated and perdeuterated [16]annulene, just as it does for the COT system. As in the case of isopropoxy-COT,⁵ intramolecular proton exchange allows the experimental observation of the energetics of ring planarization for the [16]annulene system.

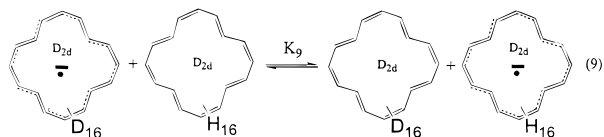
Oth and co-workers used ¹H NMR data to show that the neutral [16]annulene system undergoes rapid intramolecular proton exchange due to both bond rotation (BR), about the single bonds, and bond shift (BS).⁶ If the deuteration affects the rate of reaction 5 or 6 ($k_{BR(5)}$ or $k_{BS(6)}$) and if the geometry of the



transition state (TS) for the perturbed reaction is similar to the geometry of the anion radical, then there would be a significant contribution to the EIE in reaction 7. The free energy of



planarization, ΔG°_8 , contributing to ΔG°_7 , could be similar to the inverse EIE contribution from ΔG°_4 to ΔG°_2 . As in the cases of planar COT and various planar (PAHs),¹ a normal isotope effect for the electron transfer in the hypothetically planar [16]annulene system, reaction 9, is expected.



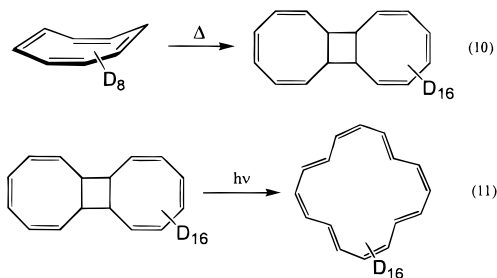
However, the comparison with COT and other PAH systems is limited due to the presence of internal protons in [16]annulene. The steric interactions of the four internal protons have a significant effect upon the characteristics of the [16]annulene system.^{6,7} Attenuation of these interactions, via replacement of the C-H bonds with shorter C-D bonds, should allow a more planar and less strained geometry for the perdeuterated systems.⁷ ¹H NMR experiments, showing increased ring current in [16]annulene-*d*₁₅ systems (Figure 1), and HF/6-31G* geometry predictions (Table 1) suggest that this is the case.^{7,8} It is reasonable to expect that the analogous interactions present in the [16]annulene anion radical would also be significantly attenuated upon deuteration and that the resulting structural alteration may influence ΔG°_7 .

As do the neutral and dianionic systems, the [16]annulene-*d*₁₆ anion radical is likely to have a larger ring current than its perdeuterated analogue.⁷ Since the angular momentum due to ring current and electron spin are coupled, perdeuteration should increase spin-orbit coupling. Stone has shown that *g*-factors of many aromatic anion radicals are dependent on spin-orbit coupling and the topology of these systems.⁹ Any alteration of the anion radical geometry, due to deuteration, would affect both the topology and the ring current and thus alter the electron spin densities and the isotropic *g*-factor of [16]annulene-*d*₁₆. Conversely, a lack of an observed deuteration effect on these physical properties would indicate that the perdeuteration has little or no effect on the geometry of the [16]annulene anion radical.

To gain insight into the nature of the molecular geometry perturbations, due to electron addition and isotopic substitution of the [16]annulene system, we were motivated to investigate ΔG°_7 , the coupling constants, and the anion radical *g*-factors of the isotopic analogues. We anticipated that this theoretical and experimental investigation of the [16]annulene system would be as insightful as were those for the [6]- and [8]annulene systems.

Results and Discussion

Samples of perdeuterated [16]annulene were synthesized via the thermal dimerization of perdeuterated [8]annulene (reaction 10) followed by photochemical ring opening of the 2 + 2 dimer (reaction 11).^{10,11} Because of the unavoidable presence of ¹H



impurity, ¹H NMR data were obtainable for the [16]annulene-*d*₁₅ present in the sample. The ¹H NMR spectrum of a mixture of [16]annulene and [16]annulene-*d*₁₅ (Figure 1), in tetrahydrofuran-*d*₈/ethanol-*d*₆ at 158 K, is described by a triplet at δ 10.55 and a singlet at δ 10.76 for the internal proton(s), respectively. The external protons of [16]annulene yield resonances consisting of a doublet of doublets at δ 5.51 and a triplet at δ 5.21. The [16]annulene-*d*₁₅ material yields singlets at δ 5.46 and δ 5.16, for the groups of eight and four protons, respectively.⁷ Resonances of further protic impurity and the minor conformer are also readily observed in the spectra (Figure 1). Consideration of the intramolecular proton exchange between the two conformations (Figure 2) is required for the complete simulation of the ¹H NMR spectra.^{6b} However, further treatment of the minor conformer is not necessary because it does not affect the reduction chemistry of [16]annulene.^{6a}

At slightly elevated temperatures (163–183 K), the resonances for the internal and external protons are broadened due to the bond rotation only, $k_{BR(5)}$.⁶ Simulations of the spectra for the protiated system at 163, 173, and 183 K, show that the rate constants for reaction 5 are 9 ± 2 , 34 ± 5 , and 110 ± 15 Hz, at these three temperatures, respectively (Figure 3). Inspection of the analogous spectra of the perdeuterated system reveals narrower resonances, indicating slower kinetics for bond rotation, $k_{BR(5)}$, in the heavier system (Figure 3). Further, an

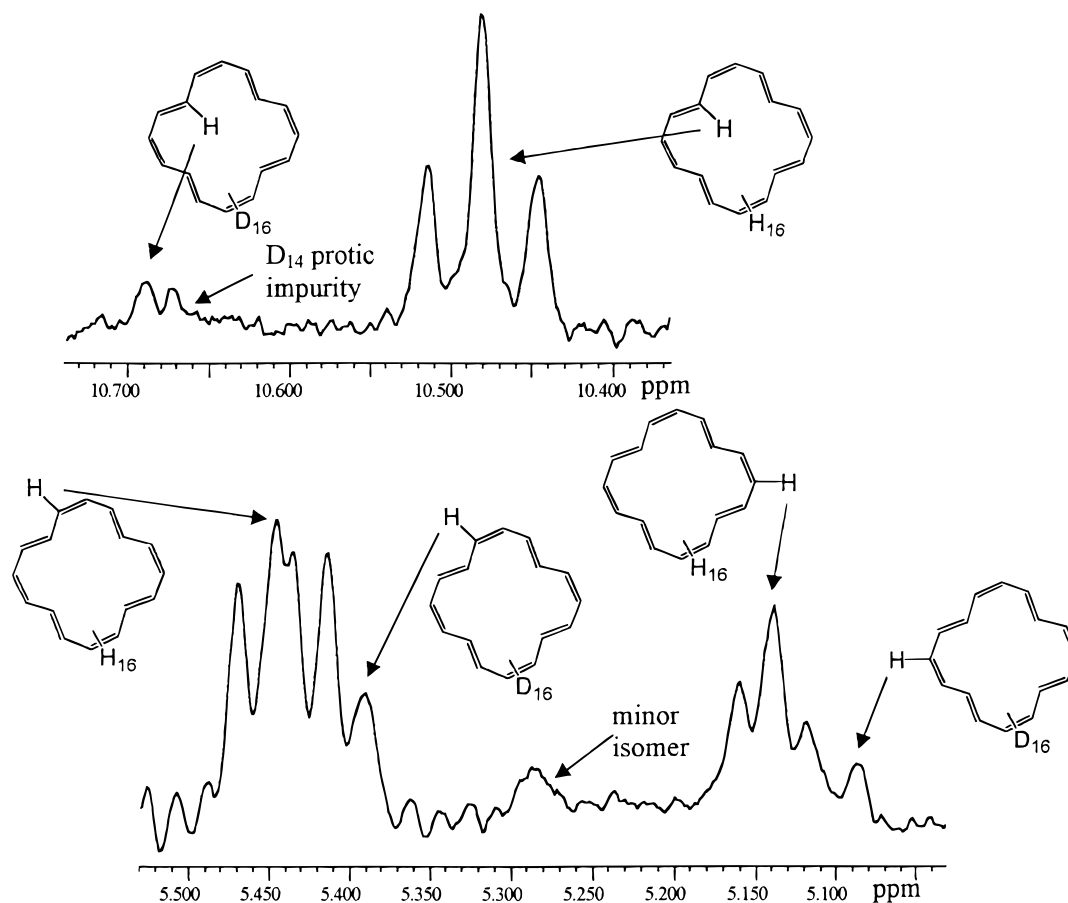


Figure 1. 400 MHz ^1H NMR spectrum of a mixture of neutral [16]annulene and [16]annulene- d_{15} , at 153 K in an ethanol- d_7 /THF- d_8 . The low-field portion (internal protons) is shown above and the high-field portion (external protons) is shown below. Note the increased paratropicity of the deuterated system. The signal at 5.4 ppm is due to the minor isomer (Figure 2). The relatively low signal-to-noise is due to the small amount of monoprotic impurity in the perdeuterated [16]annulene material. Very little [16]annulene material was added, to prevent loss of the weak resonance from [16]annulene- d_{15} present in the sample.

TABLE 1: (U)HF/6-31G* and B3LYP/6-31+G* Predictions of the Planarity of the Various Oxidation States of the [16]Annulene System As Defined by the Sum of the Dihedral Angles Shown in Figure 4

oxidation state	Φ (deg)		
	(U)HF/6-31G*		B3LYP/6-31+G*
	[16]annulene- d_{16}	[16]annulene	[16]annulene
neutral	51.10	51.92	38.02
anion	12.90	19.97	6.00
dianion	10.67	10.99	0.00

Arrhenius treatment of the data indicates that the barrier to bond rotation is higher for the perdeuterated molecule. At higher temperatures, bond shift, $k_{\text{BS}(6)}$, also contributes to the NMR line shapes and its effect must be included to adequately simulate the ^1H NMR spectra.⁶ The activation energy for bond shift was also found to be greater for the deuterated material. Thus, bond distortions occur less unfavorably in the protiated system and neither bond rotation, nor bond shift, are expected to contribute an inverse EIE to reaction 7.

Previous HF/6-31G* ab initio calculations suggest that perdeuteration of either the neutral or dianionic forms of [16]annulene will result in increased planarization of those systems.⁷ It is reasonable to expect the anion radical to undergo similar ring planarization upon deuteration. In agreement with this assumption, UHF/6-31G* calculations suggest that the sum of dihedral angles, Φ , is 7.07° smaller for the perdeuterated anion radical system (Figure 4 and Table 1).¹² This represents an even larger deuteration effect on the anion radical than on either the

neutral or the dianion species (Table 1). Further, these UHF calculations predict a relatively more planar and less strained [16]annulene- d_{16} anion radical, which should yield an inverse EIE contribution to ΔG°_7 and show perturbations of spin densities and g -factor. EPR measurements at multiple frequencies were used to test these predictions.

Hexamethylphosphoramide (HMPA) solutions of the [16]annulene materials, reduced with molar deficient amounts of sodium metal, yield anion radical solutions that are free of ion association.¹³ These solutions give EPR spectra that are characterized by three sets of coupling constants (Figure 5) that are within reasonable limits of those found by Oth in a different solvent system.^{6a} They are $a_{\text{H}} = 3.898$ G (8H), 0.697 G (4H), and 0.900 G (4H). HMPA solutions of the [16]annulene- d_{16} anion radical also exhibit highly resolved spectra that can be simulated by using coupling constants of 0.600, 0.137, and 0.108 G for the group of eight and two groups of four deuteriums, respectively.

Previously, variable- β Hückel molecular orbital theory and spectral width considerations were used to predict two small negative coupling constants corresponding to the groups of four equivalent protons and one large positive coupling constant for the remaining group of eight, in a D_{4h} anion radical geometry.⁶ However, the authors were not able to distinguish between the two small negative coupling constants. B3LYP/6-31+G* calculations, utilizing a D_{2d} anion radical geometry (predicted to be 50 cal/mol lower in energy than the D_{4h}), predict a large negative coupling constant for the group of eight protons and

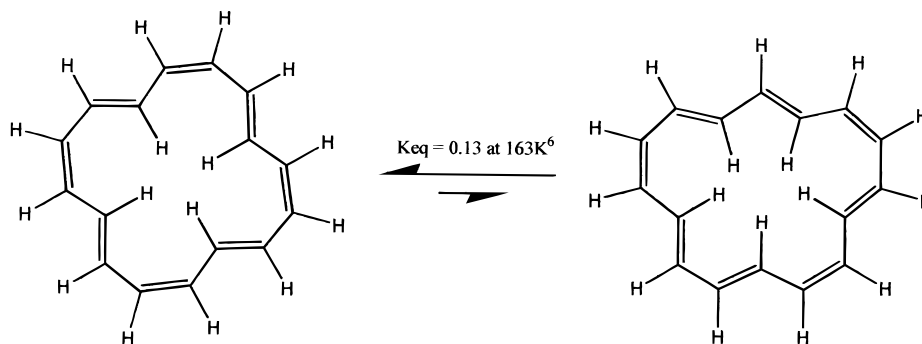


Figure 2. Neutral [16]annulene exists in two conformers. There is 7.7 times as much of the major isomer (left) at 163 K.⁶

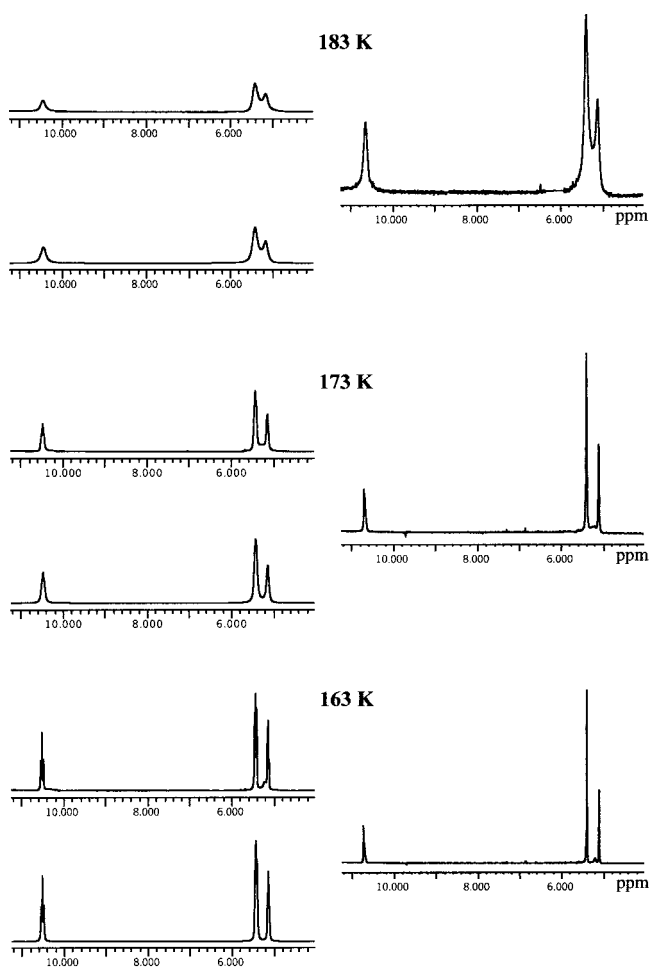


Figure 3. 400 MHz ¹H NMR of [16]annulene (left) and [16]annulene-*d*₁₅ (right) taken at 163, 173, and 183 K. Below each spectrum of [16]annulene (left) is a computer simulation that accounts for the bond rotation exchange. The values for $k_{BR(5)}$ are 9 ± 2 , 34 ± 5 , and 110 ± 15 Hz, at 163, 173, and 183 K, respectively.

two small but significantly different constants for the remaining two groups of four. This is also the case for the D_{4h} geometry. These calculations allow us to assign the smallest of the coupling constants to the internal positions. Similar DFT calculations have been shown to perform well in the prediction of EPR coupling constants.¹⁴

Error analyses of the experimental deuterium and proton coupling constants were performed via comparisons of simulations based on clearly errant values. The error for each of our reported coupling constants is within ± 0.005 G. In exact agreement with the ratio of gyromagnetic ratios, $\gamma_H/\gamma_D = 6.514$, the deuterium coupling constants are 6.51 ± 0.01 times smaller

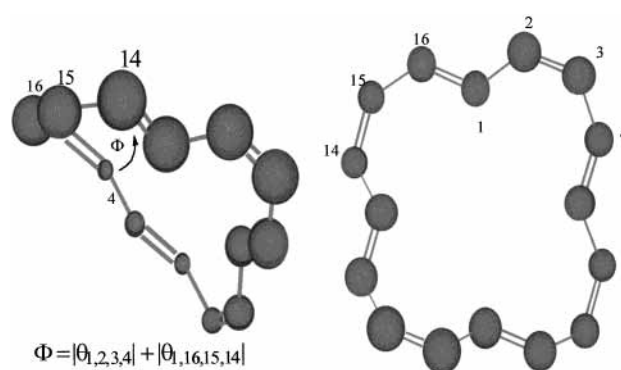


Figure 4. The divergence from planarity of the [16]annulene system is depicted by the angle Φ , which represents the sum of the absolute values of dihedral angles $\theta_{1,2,3,4}$ and $\theta_{1,16,15,14}$. On the left, the molecule is illustrated with carbons 15, 16, 1, 2, and 3 in the same plane.

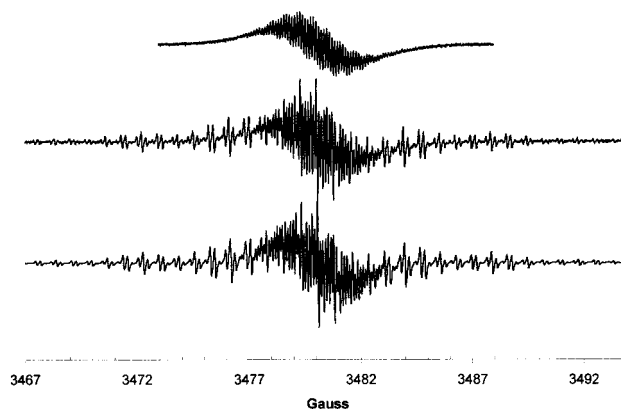


Figure 5. (Top) X-band EPR spectrum, taken at 298 K and in HMPA, of the perdeuterated [16]annulene reduced with Na metal (5% protic impurity, statistically distributed, was included for accurate simulation of the deuterated material). (Middle) X-band EPR spectrum, taken at 298 K and in HMPA, of a 35:1 (D:H) mixture of [16]annulene-*d*₁₆ and [16]annulene. The solution was reduced with a very molar deficient amount of Na metal. At the low- and high-field ends of the spectrum, unperturbed hyperfine structure of the [16]annulene anion radical is observable. (Bottom) computer simulation of the 35:1 mixture using a ratio of anion radicals, 11.7:1 (D:H). These data show that $K_7 = 3.0 \pm 0.3$. The simulation also indicates that there is no difference in g -value between the isotopic analogues.

than those found for the perprotiated material. Suggesting identical [16]annulene and [16]annulene-*d*₁₆ anion radical topologies, this equality of ratios indicates that there is no measurable perturbation of the spin densities as a result of perdeuteration. Further, W-band (94.5 GHz) EPR analysis of mixtures of the anion radicals of [16]annulene and [16]annulene-*d*₁₆ indicated that the isotropic g -factors of the two systems were identical. Thus, contrary to the UHF/6-31G* results, the EPR

TABLE 2: [16]Annulene C=C Bond Angles Predicted by B3LYP/6-31+G* Geometry Optimizations

oxidation state	C=C angle (deg)		
	α	β	γ
neutral	130.001	128.417	122.084
anion	131.528	130.695	122.988
dianion	133.435	130.783	124.999

data suggest that there could only be a very small, if any, geometry difference between the perprotiated and perdeuterated anion radicals of [16]annulene.

To address this contradiction and to more precisely analyze the system, we carried out B3LYP/6-31+G* calculations on the possible oxidation states of [16]annulene. The DFT optimization of the [16]annulene anion radical supports the EPR results in that it predicts a deviation from planarity of only 6.00° (Table 1); any possible deuteration effect on planarity would be minimal. Even smaller possible differences between the perdeuterated and perprotiated dianionic systems would then be expected. Indeed, the DFT calculations support this assumption by predicting a perfectly planar geometry for the [16]-annulene dianion (Table 1).

We previously concluded that a significant difference in planarity, and the consequent carbon p π -orbital overlap difference between the [16]annulene and [16]annulene-*d*₁₅ dianions, were responsible for their ¹H NMR chemical shift differences.^{7,8} Antithetically, a planar [16]annulene geometry requires that the difference between the [16]annulene and [16]-annulene-*d*₁₆ dianion ring currents be explained in terms of σ -framework perturbations.

Alleviation of the internal proton crowding results in carbon framework deformations, from ideal sp² hybridized C=C bond angles and C—C bond lengths, that are observable in the crystal structures of both neutral [16]annulene and [18]annulene.¹⁵ This is a reflection of the inability of those systems to completely alleviate steric interaction of their internal protons by deviation of the dihedral angles. In more planar systems, such as the anion radical and dianion systems of [16]annulene, dihedral angle perturbations should be less possible and larger σ bond angle deformations would then be required to alleviate the internal steric crowding. These predictions are supported by the B3LYP/6-31+G* obtained C=C bond angles for each of [16]annulene's oxidation states (Table 2).

Shaik and Jug with their collaborators¹⁶ have presented evidence indicating that delocalization of π electrons, and bond equalization, is enforced by the σ -framework. Hence, "relaxation" of the σ -framework of the planar [16]annulene dianion, which occurs upon deuteration, enforces greater π delocalization of the perdeuterated system.¹⁶ This increase in π delocalization yields the observed increase in diatropic ring current of the [16]-annulene-*d*₁₆ dianion.

Another relevant consideration for this system would be a deuteration effect on the positioning of each proton within the inhomogeneous induced magnetic field, which is due to both the induced ring current and the induced local currents (Figure 6d). The position of an internal proton in a [16]annulene-*d*₁₅ system may not be identical to that in a [16]annulene system. For example, any movement of a proton toward the center of the [16]annulene dianion ring, caused by deuteration of three internal positions, should result in decreased shielding, due to local currents, and increased shielding, due to the ring current (see Figure 6).¹⁷ The further upfield chemical shift of the internal proton resonance, of the [16]annulene-*d*₁₅ dianion,⁷ suggests that any effect due to the local currents is greatly offset by an

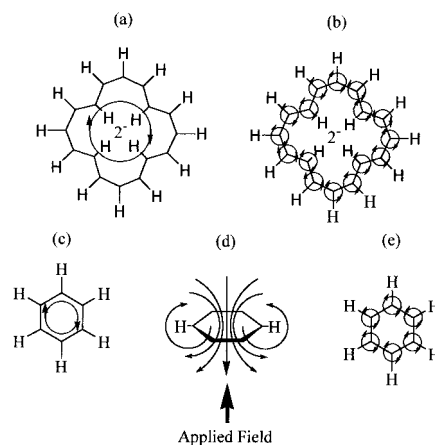


Figure 6. (a) and (c), and (b) and (e), are the induced ring currents and induced local currents, respectively, for the [16]annulene dianion and benzene. (d) shows the magnetic field due to the induced diatropic ring current in benzene. The total induced magnetic field is due to both local and ring currents. In the center of the molecules shown, the local and ring currents will oppose one another.

increased ring current effect and/or offset by repositioning within the field of the ring current. However, an external proton in a [16]annulene-*d*₁₅ dianion is not repositioned with respect to the induced field, and its slightly further downfield ¹H NMR chemical shift (relative to the internal proton resonance of [16]-annulene) must be due to an increased ring current effect. The data for the neutral systems confirms this result by showing further upfield and further downfield shifts for the external and internal proton resonances, respectively, for [16]annulene-*d*₁₅. This analysis indicates that any positional adjustment, of the protons with respect to the induced field, could not be fully responsible for the observed chemical shift differences between the ¹H NMR spectra of the [16]annulene and [16]annulene-*d*₁₅ dianion systems.

Reduction of the [16]annulene mixtures, with a molar deficient amount of sodium metal, yields the simultaneous existence of both anion radicals (C₁₆D₁₆^{•-} and C₁₆H₁₆^{•-}), thus allowing the observation of *K*₇. The equilibrium constant for reaction 7, $K_7 = [C_{16}D_{16}][C_{16}H_{16}^{•-}]/[C_{16}D_{16}^{•-}][C_{16}H_{16}]$, can be obtained from the ratio of the intensities for the EPR signal (Figure 5) for the two anion radicals, [C₁₆D₁₆^{•-}]/[C₁₆H₁₆^{•-}], and the ratio of initial neutral molecule concentrations, [C₁₆D₁₆]/[C₁₆H₁₆]. The experimental equilibrium constant, *K*₇, was found to be 3.1 ± 0.3 at 298 K. The corresponding free energy, $\Delta G^\circ_7 = -0.65 \pm 0.06$ kcal/mol, is clearly dominated by a normal EIE and is larger than normally observed for either the benzene or planar COT systems.

When supplied with B3LYP/6-31+G* vibrational frequency data for the neutral molecule and anion radical of [16]annulene, the QUIVER program³ calculates a *K*₇ of 1.27 at 298 K ($\Delta G^\circ_7 = -0.142$ kcal/mol). This is in qualitative agreement with the experimental value. The empirical and theoretical results are both consistent with the fact that the neutral [16]annulene is stabilized to a greater extent than the corresponding anion radical upon deuteration (relief of internal steric crowding). The ¹H NMR intramolecular exchange data show that there is a smaller energy difference between the bond shift transition state, which has a planar geometry (similar to that for the anion radical), and the annulene for the perprotiated molecule (reaction 6). This imparts an inverse contribution from ring planarization (ΔG°_8) to ΔG°_7 . However, the decreased steric interaction of the internal atoms of the perdeuterated [16]annulene tends to attenuate this effect. The DFT calculated value for ΔG°_7 does not account

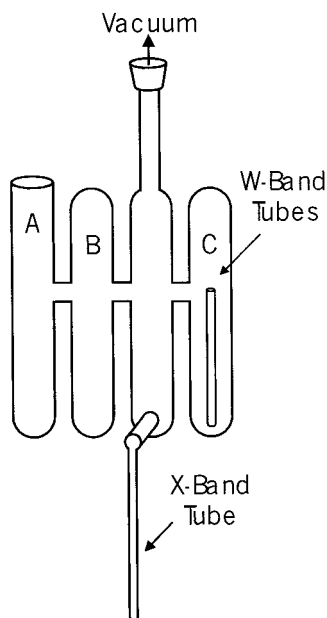


Figure 7. Glass apparatus used for the preparation and acquisition of X-band and W-band EPR spectra. The X-band tube has a 3 mm i.d. and is made of glass. Each W-band capillary tube has a 0.2 mm i.d. and is made of quartz. Many W-band tubes were prepared in each experiment.

for the effects arising from the shorter C–D bond length. This explains some of the difference between the theoretical and empirical values for ΔG°_7 .

Experimental Section

Synthesis of Materials. Starting materials for the synthesis of [16]annulene and [16]annulene- d_{16} were commercially available cyclooctatetraene (COT) and perdeuterated cyclooctatetraene (COT- d_8), which was prepared in our laboratory.¹⁰ The method of Schröder and Martin¹¹ was used to synthesize both [16]annulene and [16]annulene- d_{16} . COT- d_8 was dimerized via a 2 + 2 addition. A 5 g sample of COT- d_8 (5% protic impurity) was distilled under reduced pressure into a glass ampule that was then frozen and flame-sealed under high vacuum. This sample was then heated at 90 °C for 96 h (reaction 10). Unreacted COT- d_8 was vacuum transferred from the heavy dimerization products. A 450 W mercury cathode lamp was then used to photolyze a 100 mL ether solution containing 2 g of the unisolated dimer materials (reaction 11). The photolysis process was monitored via ^1H NMR. Once no starting material remained, the reaction was stopped. The resulting mixture was concentrated to a dark red oil and then applied to a 200 g Alumina¹⁸ column that was prepared with hexanes. [16]-Annulene- d_{16} eluted with straight hexanes. This solution was concentrated and then dissolved in a minimal amount of ether. An equal amount of cold ethanol was then added. The sample was cooled at –10 °C overnight, and crystals were collected via suction filtration and washed with cold ethanol the next day. Recrystallization, from the same solvents, was performed to enhance the purity.

Preparation of EPR Samples and Acquisition of EPR Data. Samples containing [16]annulene, [16]annulene- d_{16} , or a mixture of the two, were prepared by adding a pentane solution of the material to the apparatus, Figure 7. The pentane was then evaporated under reduced pressure. Once the apparatus was solvent-free, a small amount of sodium metal was added at point A. The apparatus was then sealed at this point. The Na metal was then distilled into tube B, creating a metal mirror, and tube

A was subsequently cut from the apparatus. HMPA, dried with potassium metal, was carefully distilled into the apparatus, which was then cut from the vacuum line. The internal solution was then gradually exposed to the metal mirror until an EPR signal was observed.

For samples containing both protiated and deuterated materials, UV/vis spectrophotometry and atmospheric pressure chemical ionization mass spectrometry (APCI MS) were used to determine exact ratios.¹⁹ UV/vis spectra were taken of dilute stock pentane solutions of the separate [16]annulenes. Because of the equality of extinction coefficients, their absorptions could be used directly as an indication of concentration. Mixtures were then prepared on the basis of the concentration data. APCI MS was used to verify the precision of this convenient method. The results of both methods were in good agreement so that further mixtures were prepared utilizing only the UV/vis method.

High field, W-band (94 GHz), experiments were conducted at the University of Illinois EPR Research Center, with a spectrometer described elsewhere.²⁰ Samples were prepared from the solutions used in the X-band study. Quartz capillaries (0.2, 0.3, 0.4, and 0.5 mm i.d., sealed at one end) were vacuum sealed into the X-band apparatus, Figure 7. Upon completion of the X-band work, the HMPA solution was poured into the side tube covering the small tubes (tube C). Breaking the apparatus in an argon atmosphere resulted in the filling of the quartz tubes. Via a rubber septum, the small quartz tubes were individually attached to a vacuum line. The samples were subsequently frozen, evacuated, and flame-sealed. It was found through trial and error that the 0.2 i.d. tubes yielded the best Q value for the instrument and therefore the best signal-to-noise spectra. This was presumably due to the high dielectric losses in the HMPA solvent at 94 GHz; signal-to-noise was worse with larger diameter tubes.

Instrumental Parameters. Typical X-band EPR acquisition parameters: data were obtained using a Bruker EMX spectrometer operating at 9.8 GHz; modulation frequency, 60.00 kHz; modulation amplitude, 0.05 G. Typical W-band EPR acquisition parameters: data were obtained on a custom EPR spectrometer²⁰ operating at 94.5 GHz; modulation frequency, 60 kHz; modulation amplitude, 0.05 G.

The parameters for the APCI MS were as follows: drying gas flow, 2.0 L/min; nebulizer pressure, 60 psi; drying gas temperature, 300 °C; vaporizer temperature, 250 °C; capillary voltage, 2000 V; corona current, 80 μA . The solvent was acetonitrile, and the concentration was about 5 μM .

NMR spectra were recorded on a Varian Mercury 400 MHz spectrometer with a Varian model L900 temperature controller. The NMR simulations were generated with the gNMR v.4.0 program.²¹

EWSim and EWPlot were used to simulate the EPR spectra.²²

Computational Methodology. Similar in method to our previous work,⁷ initial geometry optimization of the [16]-annulene system was carried out using the PM3 model in the Spartan program.²³ The obtained C–H bond distances were then constrained to the average values of their respective positions. C–D bonds were simulated by constraining the C–H bonds to 0.01 Å less than their calculated values.^{24,25} Each structure was then further optimized using the Hartree–Fock (HF) model with the 6-31G* basis set. Using the unrestricted HF model, and the same basis set, the procedure was carried out for the anion radical systems. The relevant data are shown in Table 1.

Advanced calculations were carried out with the 6-31+G* basis set²⁶ employing the three-parameter functional of Becke and incorporating the nonlocal correlation functional of Lee,

Yan, and Parr.²⁷ Geometry optimizations of [16]annulene, [16]-annulene anion radical, and [16]annulene dianion were performed at the B3LYP/6-31+G* level utilizing the gradient packages as incorporated in the Gaussian 94 suite of programs.²⁸ Vibrational analyses were subsequently performed at each geometry to verify that, indeed, a local minimum on the potential energy surface had been found. Isotope effects were evaluated from the Cartesian force constants obtained from the vibrational analyses by the program QUIVER.³ EPR hyperfine coupling constants for the [16]annulene radical anion were calculated from the obtained Fermi contact values.¹⁴

Acknowledgment. C.D.S. thanks the National Science Foundation (Grant 9617066) for support of this work. The Illinois EPR Research Center is supported by the National Institutes of Health (RR01811).

References and Notes

- (1) Stevenson, C. D.; Espe, M. P.; Reiter, R. C. *J. Am. Chem. Soc.* **1986**, *108*, 533. (b) Stevenson, C. D.; Espe, M. P.; Reiter, R. C. *J. Am. Chem. Soc.* **1986**, *108*, 5760. (c) Lauricella, T. L.; Pescatore, J. A.; Reiter, R. C.; Stevenson, R. D.; Stevenson, C. D. *J. Phys. Chem.* **1988**, *92*, 3687. (d) Stevenson, C. D.; Sturgeon, B. E.; Vines, S. K.; Peters, S. J. *J. Phys. Chem.* **1988**, *92*, 6850. (e) Stevenson, C. D.; Reidy, K. A.; Peters, S. J.; Reiter, R. C. *J. Am. Chem. Soc.* **1989**, *111*, 6578. (f) Stevenson, C. D.; Sturgeon, J. *Org. Chem.* **1990**, *55*, 4090. (g) Stevenson, C. D.; Halvorsen, T. D.; Reiter, R. C. *J. Am. Chem. Soc.* **1993**, *115*, 12405.
- (2) Stevenson, C. D.; Peters, S. J.; Reidy, J. A.; Reiter, R. C. *J. Org. Chem.* **1992**, *57*, 1877.
- (3) Bigeleisen, J.; Mayer, M. G. *J. Chem. Phys.* **1947**, *15*, 261. (b) Wolfsburg, M. *Acc. Chem. Res.* **1972**, *5*, 225. (c) Saunders: M.; Laidig, K. E.; Wolfsberg, M. *J. Am. Chem. Soc.* **1989**, *111*, 8989.
- (4) Hrovat, D. A.; Hammons, J. H.; Stevenson, C. D.; Borden, W. T. *J. Am. Chem. Soc.* **1997**, *119*, 9523.
- (5) Stevenson, C. D.; Brown, E. C.; Hrovat, D. A.; Borden, W. T. *J. Am. Chem. Soc.* **1998**, *120*, 8864.
- (6) Oth, J. F. M.; Baumann, H.; Gilles, J.-M.; Schröder, G. *J. Am. Chem. Soc.* **1972**, *94*, 3498. (b) Oth, J. F. M. *Pure Appl. Chem.* **1971**, *25*, 573.
- (7) Stevenson, C. D.; Kurth, T. L. *J. Am. Chem. Soc.* **1999**, *121*, 1623.
- (8) Haddon, R. C. *Acc. Chem. Res.* **1988**, *21*, 243.
- (9) Stone, A. J. *Mol. Phys.* **1963**, *6*, 509. (b) Stone, A. J. *Proc. R. Soc. A* **1963**, *271*, 424.
- (10) Reppe, W.; Schlichting, O.; Klager, K.; Toepel, T. *Annalen* **1948**, *560*, 1. (b) Stevenson, C. D.; Burton, R. D.; Reiter, R. C. *J. Am. Chem. Soc.* **1992**, *114*, 399. (c) Stevenson, C. D.; Burton, R. D.; Reiter, R. C. *J. Am. Chem. Soc.* **1992**, *114*, 4514.
- (11) Schröder, G.; Martin, W.; Oth, J. F. M. *Angew. Chem., Int. Ed. Engl.* **1967**, *6*, 870.
- (12) Φ relates to the overlap of the π orbitals and has been described in terms of the π orbital axis vector (POAV) by Haddon.⁸
- (13) Levin, G.; Jagur-Grodzinski, J.; Szwarc, M. *J. Am. Chem. Soc.* **1970**, *92*, 2268. (b) Stevenson, C. D.; Echegoyen, L.; Lizardi, L. R. *J. Phys. Chem.* **1972**, *76*, 1439.
- (14) Batra, R.; Giese, B.; Spichty, M.; Gescheidt, G.; Houk, K. N. *J. Phys. Chem.* **1996**, *100*, 18371.
- (15) Bregman, J.; Hirschfeld, F. L.; Rabinovich, D.; Schmidt, G. M. *J. Acta Crystallogr.* **1965**, *19*, 227.
- (16) Shaik, S. S.; Hiberty, P. C.; Ohanessian, G.; Lefour, J.-M. *J. Phys. Chem.* **1988**, *92*, 5086. (b) Jug, K.; Koster, A. M. *J. Am. Chem. Soc.* **1990**, *112*, 6772.
- (17) Barfield, M.; Grant, D. M.; Ikenberry, D. *J. Am. Chem. Soc.* **1975**, *97*, 6956.
- (18) Aldrich, activated, neutral, Brockmann 1, deactivated with 6 mL of H₂O/100 mL of alumina.
- (19) We would like to thank Dr. James Webb, Illinois State University, for his invaluable expertise in carrying out of the APCI MS experiments. This method was used so that molecular ion concentrations could be accurately observed.
- (20) Wang, W.; Belford, R. L.; Clarkson, R. B.; Daub, R. B.; Forrer, R. B.; Nilges, M. J.; Timken, M. D.; Watzak, T.; Thurnauer, M. C.; Norris, J. R.; Morris, A. C.; Zwing, Y. *Appl. Magn. Reson.* **1994**, *6*, 195.
- (21) gNMR, v. 4.0, Cherwell Scientific Publishing Limited, Oxford, U.K., 1997.
- (22) EWPlot v. 3.2 and EWSim v. 4.0, Scientific Software Services, Normal, IL, 1997.
- (23) Spartan v. 5.0, Wave function Inc., Irvine, CA, 1997.
- (24) For naphthalene, X-ray crystallography reveals a reduction of the C–L (L = H or D) bond length from 1.085 (C–H) to 1.073 (C–D) Å; Berger, S.; Kunzer, H. *Tetrahedron* **1983**, *39*, 1327. (b) For other cases of isotopic bond length reduction, see: Bartell, L. S.; Roth, E. A.; Hollowell, C. D. *J. Chem. Phys.* **1965**, *42*, 2683. Melander, L.; Saunders: W. H. *Reaction Rates of Isotopic Molecules*; Wiley: New York, 1980; pp 189–197.
- (25) This treatment of deuterated systems is similar to that used by: Zuilhoff, H.; Lodder, G.; van Mill, R. P.; Mulder, P. P. J.; Kage, D. E.; Reiter, R. C.; Stevenson, C. D. *J. Phys. Chem.* **1995**, *99*, 3461.
- (26) Harihan, P. C.; Pople, J. A. *Theor. Chim. Acta* **1973**, *28*, 213. (b) Clark, T.; Chandrasekhar, J.; Spitznagel, G. W.; Schleyer, P. v. R. *J. Comput. Chem.* **1983**, *4*, 294.
- (27) Becke, A. D. *J. Chem. Phys.* **1993**, *98*, 5648. (b) Lee, C.; Yang, W.; Parr, R. G. *Phys. Rev. B* **1988**, *37*, 785.
- (28) Frisch, M. J.; Trucks, G. W.; Schlegel, H. B.; Gill, P. M. W.; Johnson, B. G.; Robb, M. A.; Cheeseman, J. R.; Keith, T.; Petersson, G. A.; Montgomery, J. A.; Raghavachari, K.; Al-Laham, M. A.; Zakrzewski, V. G.; Ortiz, J. V.; Foresman, J. B.; Peng, C. Y.; Ayala, P. Y.; Chen, W.; Wong, M. W.; Andres, J. L.; Replogle, E. S.; Gomperts, R.; Martin, R. L.; Fox, D. J.; Binkley, J. S.; Defrees, D. J.; Baker, J.; Stewart, J. P.; Head-Gordon, M.; Gonzalez, C.; Pople, J. A. *Gaussian 94*, Revision B.3; Gaussian Inc.: Pittsburgh, PA, 1995.